

## Modification of Silica Coated on Iron Sand Magnetic Material with Chitosan for Adsorption of Au(III)

Muflikhah<sup>1,\*</sup>, Bambang Rusdiarso<sup>1</sup>, Edy Giri Rachman Putra<sup>2</sup>, and Nuryono<sup>1</sup>

<sup>1</sup>Department of Chemistry, Faculty of Mathematics and Natural Sciences, Universitas Gadjah Mada, Sekip Utara PO BOX BLS 21 Yogyakarta 55281, Indonesia

<sup>2</sup>Polytechnic Institute of Nuclear Technology-Nuclear Energy Agency, Jl. Babarsari, Yogyakarta, Indonesia

Received February 27, 2017; Accepted July 20, 2017

### ABSTRACT

Modification of silica coated on magnetic material iron sand with chitosan for adsorption of Au(III) has been carried out. Magnetic material (MM) from iron sand was separated using an external magnet, washed with water and HF solution 10%. MM-silica-chitosan material (MMSC) was synthesized via sol gel process and the product was characterized with Fourier Transform Infrared (FT-IR) spectrophotometer, X-ray diffractometer, scanning electron microscopy and energy dispersive X-ray, thermogravimetric analysis, and vibration sample magnetometer. Additionally, the effect of pH on the stability of MMSC has also been tested. The adsorption of Au(III) on MMSC was proceeded in a batch system with variation of pH, contact time, and concentration of absorbate. Adsorbent was separated using external magnet and concentration of Au(III) not adsorbed was analyzed using Atomic Absorption Spectrometer. Characterization result indicated that MMSC was successfully synthesized. Adsorption of Au(III) on MMSC followed pseudo second-order kinetic model with the value of adsorption rate constant ( $k$ ) of  $4.10 \times 10^{-3} \text{ g mg}^{-1} \text{ min}^{-1}$  and adsorption isotherm fixed with Langmuir model with the adsorption capacity ( $q_{\text{max}}$ ) of  $149.25 \text{ mg g}^{-1}$ .

**Keywords:** silica; chitosan; iron sand; Au(III) adsorption

### ABSTRAK

Modifikasi silika terlapis pada bahan magnetik pasir besi dengan kitosan untuk adsorpsi Au(III) telah dilakukan. Bahan magnetik (MM) dari pasir besi dipisahkan menggunakan medan magnet eksternal, selanjutnya dicuci dengan aquadest dan larutan HF 10%. MM-silika-kitosan (MMSC) disintesis melalui proses sol-gel dan produk dikarakterisasi menggunakan spektrofotometer Fourier Transform Infrared (FT-IR), difraktometer sinar-X, scanning elektron mikroskopi dan energi dispersive X-ray, analisis termogravimetri, dan vibration sample magnetometer. Selain itu, pengaruh pH terhadap kestabilan MMSC juga diuji. Adsorpsi Au(III) terhadap MMSC dilakukan dalam sistem batch dengan variasi pH, waktu kontak, serta konsentrasi absorbat. Adsorben dipisahkan menggunakan magnet eksternal dan konsentrasi Au(III) yang tidak teradsorpsi dianalisis menggunakan Spektrometer Serapan Atom. Hasil karakterisasi mengindikasikan bahwa MMSC telah berhasil disintesis. Adsorpsi Au(III) pada MMSC mengikuti model kinetika orde-kedua semu dengan nilai konstanta adsorpsi ( $k$ ) adalah  $4,10 \times 10^{-3} \text{ g mg}^{-1} \text{ men}^{-1}$  dan isotherm adsorpsi sesuai dengan model Langmuir dengan kapasitas adsorpsi ( $q_{\text{max}}$ ) of  $149,25 \text{ mg g}^{-1}$ .

**Kata Kunci:** silika; kitosan; pasir besi; adsorpsi Au(III)

### INTRODUCTION

Gold is a noble metal that widely used in various fields, including health, industrial electronics, jewelry, and even in food and drink [1]. The relative abundance of gold in the ore is estimated about 0.004 g/ton [2], which is less than gold content in electronic waste (e-waste) [3]. Nowadays, the consumption of gold has increased, this condition encourage researchers to develop gold isolation method. There are several methods to uptake gold from aqueous solution, such as solvent extraction, precipitation and adsorption [4].

Among those methods, adsorption has been considered to be promising one for gold recovery due to high efficiency and can be applied in low concentration [5-6].

In the development of the adsorbent, silica gel has been widely studied because it has large surface area and stable in acidic medium [7-8]. Silica gel surface consists of siloxane (Si-O-Si) and silanol (Si-OH) groups that allow to be modified through covalent binding with surface functional groups such as -CN, -SH, and -NH<sub>2</sub> [9]. Modification of silica surface can increase the adsorption effectivity and selectivity of the

\* Corresponding author.  
Email address : muflikhah@mail.ugm.ac.id

metal ions [10]. Adsorption of Au(III) by silica modified with organic compounds containing amine groups provides greater capacity [11], which increases along with the increasing amount of amine groups on the silica surface [12].

Chitosan (N-deacetylated form of chitin) is renewable biopolymer that has attracted great attention as a bio-sorbent due to its significant adsorption potential for the removal of heavy metal ions [13]. The presences of the amine group and the hydroxyl group that are widely available in chitosan makes chitosan to be able to form chelates with almost all metal ions [14]. However, chitosan has disadvantages when it is used directly as an adsorbent because of its solubility in acidic solution. Amine and hydroxyl groups in chitosan are active sites and allow for modification with inorganic material such as silica to form a hybrid organic-inorganic material with better performance, i.e. more stable and showing higher adsorption capacity. Silanol groups of silica can form covalent bonding with hydroxyl group (C-6) of chitosan [15]. However, other interaction such as hydrogen bonding and electrostatic attraction also play a role in the formation of hybrid material [16].

Adsorbent in a batch system is usually collected via centrifugation or filtration, which is not effective [5]. Development of adsorbent with magnetic property offers easier adsorbent separation from aqueous solution using an external magnet [17] and synthetic magnetic materials such as magnetite ( $\text{Fe}_3\text{O}_4$ ) usually is used as magnetic source. However, in the fabrication of synthetic magnetic materials generates new waste. Iron sand can be used as an alternative source of magnetic materials, because the main composition of iron sand is oxides of iron such as  $\text{Fe}_3\text{O}_4$ , hematite ( $\alpha\text{-Fe}_2\text{O}_3$ ), and maghemite ( $\gamma\text{-Fe}_2\text{O}_3$ ) [18].

In this paper, we report modification of magnetic material iron sand coated silica with chitosan and adsorption characteristics of Au(III) in a batch system. Synthesis was carried out via sol-gel process in an ambient temperature. The influence of initial pH of the Au(III) was investigated, Langmuir and Freundlich [19] isotherms were used to evaluate the equilibrium adsorption data and the adsorption kinetics was studied using pseudo first order and pseudo second order models [20].

## EXPERIMENTAL SECTION

### Materials

Iron sand sample was obtained from coast of Bugel, Kulon Progo, Yogyakarta, Indonesia. Magnetic material (MM) was separated from iron sand with Neodymium permanent magnet, grounded to 200 mesh and washed using water to remove impurities in MM iron

sand, then washed with HF solution 10% to reduce the silica content in BM (because the BM is subsequently coated with silica, so there will be no competition or interference between the silica coating with the silica contained in the magnetic material). After treatment with HF solution, magnetic material was rinsed with water till neutral and then dried at temperature 80 °C for 4 h. Sodium silicate ( $\text{Na}_2\text{SiO}_3$ ) solution (25-27%  $\text{SiO}_2$ ), acetic acid, and ammonium hydroxide, HCl, HF, and  $\text{HAuCl}_4$  1000  $\text{mg L}^{-1}$  solution were purchased from Merck. Chitosan (degree of deacetylation  $\geq 90\%$ ) was purchased from CV Chemix Yogyakarta. Chitosan solution that used in this experiment was obtained by dissolving amount of chitosan in 1% acetic acid.

### Instrumentation

The equipments were used in this research: stirrer, external magnet (Neodymium, grade N35, size 40 mm x 30 mm x 10 mm), oven, grinder, pH-meter, shaker have been used on synthesis and adsorption process. An FTIR spectrometer (Nicolet Avatar 360 IR), an X-Ray Diffractometer (XRD) Rigaku Multiplex, a scanning electron microscope (SEM)/energy-dispersive X-ray (EDX) spectroscopy (JEOL JSM-6360LA), a vibrating sample magnetometer (VSM) (OXFORD 1,2T), and Thermogravimetric analysis (TGA) NETZSCH STA 449F1 Jupiter were used for characterization of the produced materials. The stability of chitosan on the iron sand magnetic material coated silica was examined by measuring the absorbance of dissolved chitosan using UV-Vis spectrometer (Shimadzu) [21]. Iron ion concentration released from the materials and Au(III) in supernatant were determined using a flame atomic absorption spectrophotometer (FAAS, Analytic Jena 300).

### Procedure

#### Synthesis and characterization

Synthesis of silica-chitosan hybrid coated on iron sand magnetic material (MMSC) has been done via sol-gel process. About 0.5 g of MM, 1 mL of sodium silicate solution, and 30 mL chitosan solution were used in the synthesis process to get mole ratio of Fe in MM to silica 1:1. In this study % w/v of chitosan solution was varied 1, 2, and 3%. MM was activated with 1 mL of HCl 1 M, then mixed with 1 mL (3 mmol) sodium silicate solution and deionized water. The mixture was stirred with addition of HCl 1 M solution drop wise to reach the pH of 10, then immediately was poured into chitosan solution and stirred for 1 h at a room temperature till homogeneous.  $\text{NH}_4\text{OH}$  0.5 M was added into the mixture drop wise to get the pH of 7, and gelling occurred. The resulted gel was left

overnight in a close container, then washed with deionized water and dried at 60 °C for 24 h. The solid material was grounded, washed and separated with an external magnetic field. Material attracted was dried at 60 °C for 6 h then characterized with FT-IR spectrophotometer, XRD, SEM-EDX TGA, and VSM.

### Adsorption

Adsorption was carried out in a batch system by adding 20 mg of adsorbent in 10 mL of Au(III) solution (100 mg L<sup>-1</sup>) at various pHs from 1 to 6. The mixture was shaken for 2 h, then adsorbent was separated with a magnet. The concentration of Au(III) in supernatant was analyzed with FAAS. The concentration of Au(III) adsorbed was calculated using equation

$$Q = (C_o - C_e)V/W \quad (1)$$

where Q represents the amount of the Au(III) adsorbed (mg g<sup>-1</sup>); C<sub>o</sub> and C<sub>e</sub> are the initial and final concentration of the ion (mg L<sup>-1</sup>), respectively; V is volume of adsorbate (L); and W is the mass of the adsorbent (g).

An analog procedure at optimum pH was carried out with varying contact time (5, 10, 30, 60, 120, and 240 min) to study the kinetics of the adsorption. The pseudo-first order and pseudo-second order kinetic models were examined and rate constants were calculated. The similar adsorption at various initial concentrations of Au(III) solution in a range 50-300 mg L<sup>-1</sup> at constant pH and contact time was conducted. The resulted data was evaluated with Langmuir and Freundlich equations to determine the adsorption capacity [19].

## RESULT AND DISCUSSION

### Characteristics of Silica-Chitosan Hybrid Coated on Iron Sand Magnetic Material

#### Functional group

In the hybridization of silica and chitosan, chitosan solution which used referred to the previous research with the concentration in a range of 1-3% [13,22-23]. This is related to the viscosity of chitosan solution, where the more viscous solution, the mobility of molecules decreases. In this research, a preliminary study of chitosan with variation of 1-3% (weight/volume) was conducted to obtain optimum composition of chitosan solution used for the next stage. Weight of the product increased along with the greater percent of chitosan added. However, the use of chitosan 3% gave too viscous solution led to inhomogeneous mixture of MM and sodium silicate, and part of materials were lost during washing. The utilization of chitosan solution of 1 and 2% generated more homogeneous mixture.

FTIR spectrophotometric analysis was carried out in order to verify the presence of silica coating and attached chitosan. Synthesis of MMSC using sol-gel

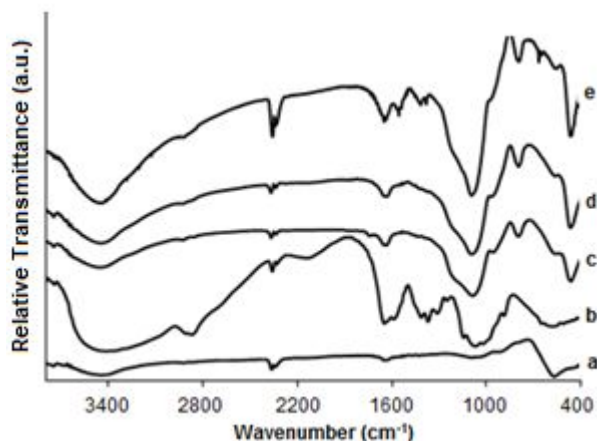


**Fig 1.** FTIR spectra of (a) MM (b) pure chitosan (c) MMS (d) MMSC 1% (e) MMSC 2%

method involved polymerization of silica, through siloxane bond (Si-O-Si) formation. The presence of silica coated on the magnetic material is showed with the appearance of specific absorption of Si-O-Si vibration in FT-IR spectra of MM-silica (MMS) which not appear in MM FT-IR spectra. In the sol-gel process, synthesis of chitosan-silica hybrid, the mixture of MM-silica was added to chitosan solution where hydrolysis and condensation take place. The FTIR spectra of MM, MMS and MMSC are shown in Fig. 1. Based on the obtained FTIR spectra, identified characteristic bands at 571 cm<sup>-1</sup> which represents to stretching vibration of Fe-O in magnetite. Peaks at 1627 cm<sup>-1</sup> and 3448 cm<sup>-1</sup> are attributed to bending and stretching vibration of OH groups on the surface of the magnetic material. The coating of silica onto MM surface was confirmed by the band at 1088 cm<sup>-1</sup> due to stretching of Si-O-Si with high intensity compare to bare MM FT-IR spectra. The absorption peak of stretching symmetry vibration of Si-O is shown at 795 cm<sup>-1</sup>. The absorption peaks of Fe-O and Si-O also appear in the FTIR spectra of MMSC.

FTIR spectra of MMSC with chitosan 1 and 2% (MMSC 1% and MMSC 2%) showed the absorption peak at 1641 and 1558 cm<sup>-1</sup> due to vibration of C=O (amide I) and N-H (amide II), respectively. The wide characteristic absorption band for chitosan at 3454 cm<sup>-1</sup> is attributed to O-H and N-H vibrations. Stretching vibration of C-C appears at 1413 cm<sup>-1</sup> and C-H bending vibration at 1380 cm<sup>-1</sup>. Absorption at 1080-1090 cm<sup>-1</sup> is derived from the vibrations of C-O and Si-O. The characteristic peaks in FTIR spectra of MMS, MMSC 1%, and MMSC 2% confirm the success of modifying chitosan over silica coated on MM. Possible interaction in MMSC structure is shown in Fig. 2. FTIR spectra of MMSC 2% provides higher intensity of characteristic peaks of chitosan than that of MMSC 1%, indicating that using 2% chitosan solution is an optimum composition of the silica modification. Therefore, MMSC

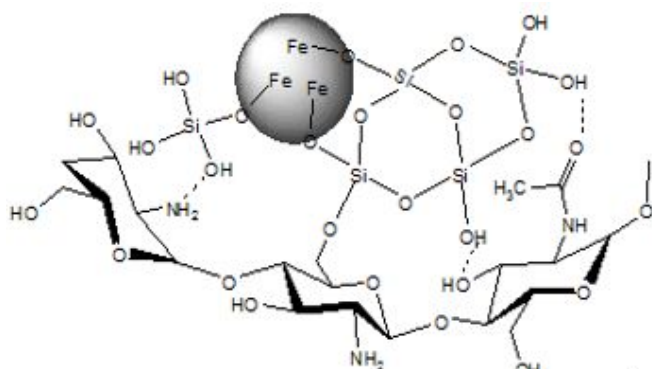


Fig 2. Structural model of MM-silica-chitosan

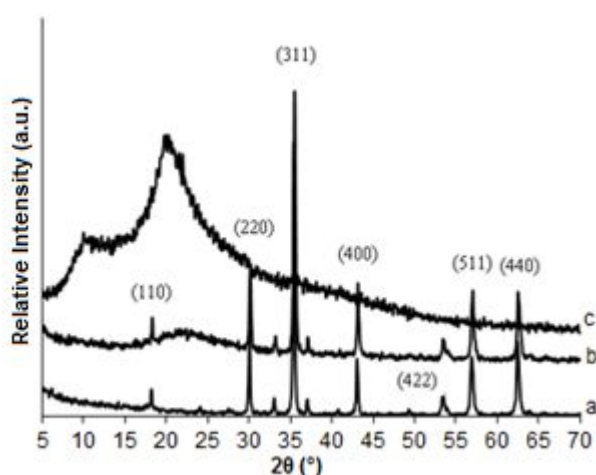


Fig 3. XRD pattern of (a) MM (b) MMSC (c) Chitosan

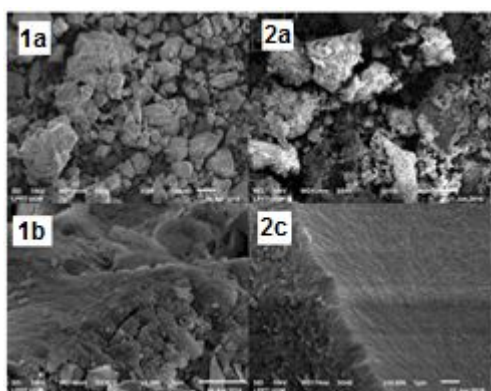


Fig 4. SEM image of (1a, b) MM-silica surface (2a, b) MMSC surface

Table 1. Percentage of carbon, oxygen, nitrogen, silica, and iron atom in coated MM

Materials	% Atom				
	C	N	O	Si	Fe
MMS	14.93	4.70	55.48	20.58	4.32
MMSC	27.93	8.05	46.02	15.65	2.34

2% has been chosen for application as adsorbent of Au(III).

### Structure and morphology

XRD pattern of MMSC is shown in Fig. 3. Wide peak at  $2\theta$  from  $18-27^\circ$  corresponds to diffraction of the silica-chitosan. Diffraction peaks of silica commonly appear at  $2\theta = 17.8^\circ; 19.1^\circ; \text{ and } 20.6^\circ$  [15]. Peaks of silica at XRD pattern MMSC are shown in  $2\theta = 18.30^\circ$  and  $18.26^\circ$ . Peak of chitosan on MMSC is shown at  $21.14-22.36^\circ$ . Compared with pure chitosan diffraction ( $2\theta = 20-22^\circ$ ), emerge a decline of chitosan crystallinity on MMSC. This is because chitosan has interacted with silica, where the intrinsic hydrogen bonds between the amine and hydroxyl groups broke up and the bond of hydroxyl and amine groups of chitosan with polysiloxane group of silica formed [8]. Peak at  $2\theta 10^\circ$  of pure chitosan is not already visible on the XRD pattern of product. It is assumed that chitosan binds covalently to silica [24]. The characteristic peaks of MM do not significantly change, which indicates the coating process do not damage the structure of magnetite.

Surface morphology of MMS and MMSC is shown in Fig. 4. The SEM photograph of surface morphology shows an irregular shape with size ranging from  $40-192 \mu\text{m}$ . The surface of chitosan modified material looks more rugged than MM-silica surface. The result analysis with EDS data for content of carbon, oxygen, nitrogen, silica, and iron in products is shown in Table 1. The percentage of the carbon and nitrogen in MMSC is higher than that in MM-Silica (MMS). The presence of nitrogen atom in MMSC indicates that chitosan is contained in the product. The decline in the percentage of iron shows that MM was coated. The percentage of silica in the MMSC surface also decreases, indicating the surface of the material is dominated by chitosan.

### Magnetic properties

The amount of silica-chitosan coated on MM may affect magnetic property of the product. Magnetic property analysis has been carried out with VSM, a power of the external magnetic field has been applied to produce a hysteresis curve describing the magnetic properties of samples. This curve resulted from analysis of coated and un-coated MM is expressed in Fig. 5. The magnetic parameters including saturation field value ( $M_s$ ), coercivity field ( $H_c$ ), and permanent magnetization ( $M_r$ ) have been calculated and presented in Table 2. The hysteresis curve represents the energy required for magnetization. From Fig. 8 seems that all materials investigated give small curve area, indicating low energy for magnetization and are classified as soft magnet. Coating magnetic material with chitosan-silica hybrid leads to decrease of magnetization. From Table 4, based on the  $M_s$  value, it

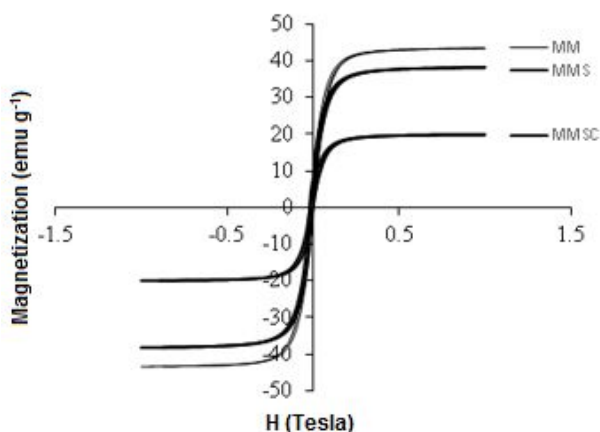


**Fig 5.** VSM hysteresis curve of coated and un-coated magnetite materials

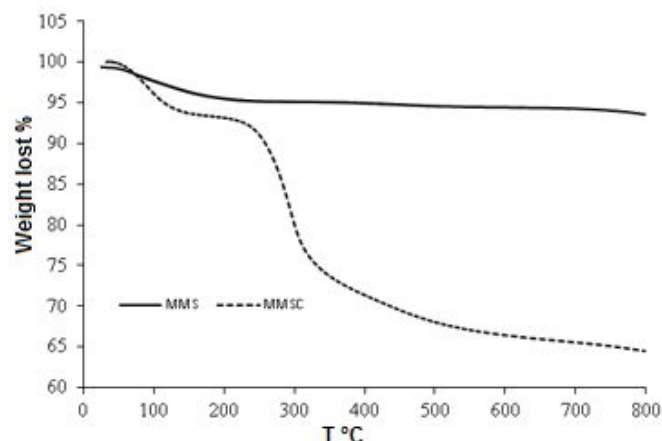


**Fig 6.** Thermogram of MMS and MMSC

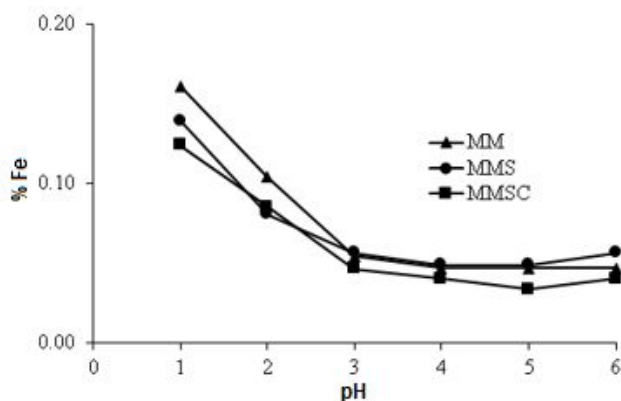


**Fig 7.** Percentage of Fe that released from MM, MMS, and MMSC

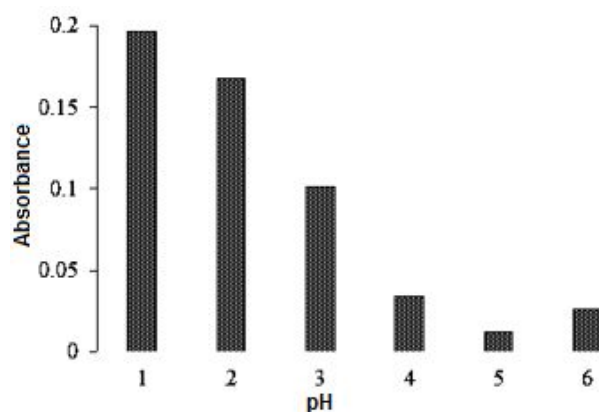


**Fig 8.** UV-Vis absorbance of MMSC

**Table 2.** Magnetic parameters of magnetic materials

Material	Ms (emu g <sup>-1</sup> )	H (Tesla)	Mr (emu g <sup>-1</sup> )
MM	43.400	0.0005	4.017
MMS	38.231	0.0193	4.535
MMSC	20.157	0.0018	2.274

can be seen that coated-MM gives lower magnetic property than un-coated one. Magnetivity of single layer coating (MM-silica) is higher than multilayer coating (MMSC).

### Thermal analysis

TGA analysis was performed to determine the composition and to predict thermal stability of the material. Analysis was conducted for MMS and MMSC. Analysis was performed with a flow rate of 50 mL min<sup>-1</sup> at nitrogen atmospheric condition. Samples were placed in an aluminum sample container and analyzed from a room temperature up to 800 °C. The amount of organic and inorganic materials contained in the product can be predicted from the percentage of weight lost displayed in TGA curve [25].

TGA curve of the materials synthesized is shown in Fig. 6. At low temperature, weight loss from 50 up to 170 °C (endothermic peak) corresponds to the evaporation of physically adsorbed water. Weight loss at a temperature 200-800 °C at MMS is attributed to the escape of water due to formation of siloxane groups from silanol groups [26]. Chitosan started to undergo rapid thermal destruction at 200-300 °C [27]. Decomposition of the polymer chain in MMSC occurs rapidly at temperature range of 243.5-330 °C about 16.66%. Decomposition continues slowly until temperature of 700 °C with weight loss about 10.11%. Decomposition phase II and III was derived from organic material (chitosan). Thermal destruction of chitosan occurs at a temperature of 200-300 °C is associated with oxidation of -NH<sub>2</sub> and -CH<sub>2</sub>OH. At temperature of 600 °C decarboxylation of oxidized -CH<sub>2</sub>OH groups, termination glycoside bond, and release of nitrogen oxides from oxidized amino groups occur [28]. At temperatures above 700 °C the remaining weight is estimated from inorganic material silica and MM about 66%. All of the characterization

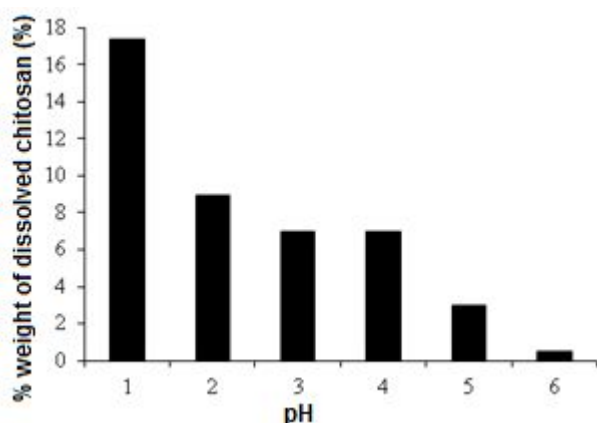


Fig 9. % weight of chitosan that dissolved in various pH

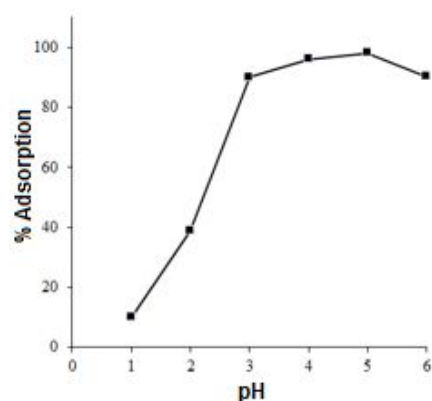


Fig 10. Effect of pH on Au(III) adsorption by MM-silica-chitosan

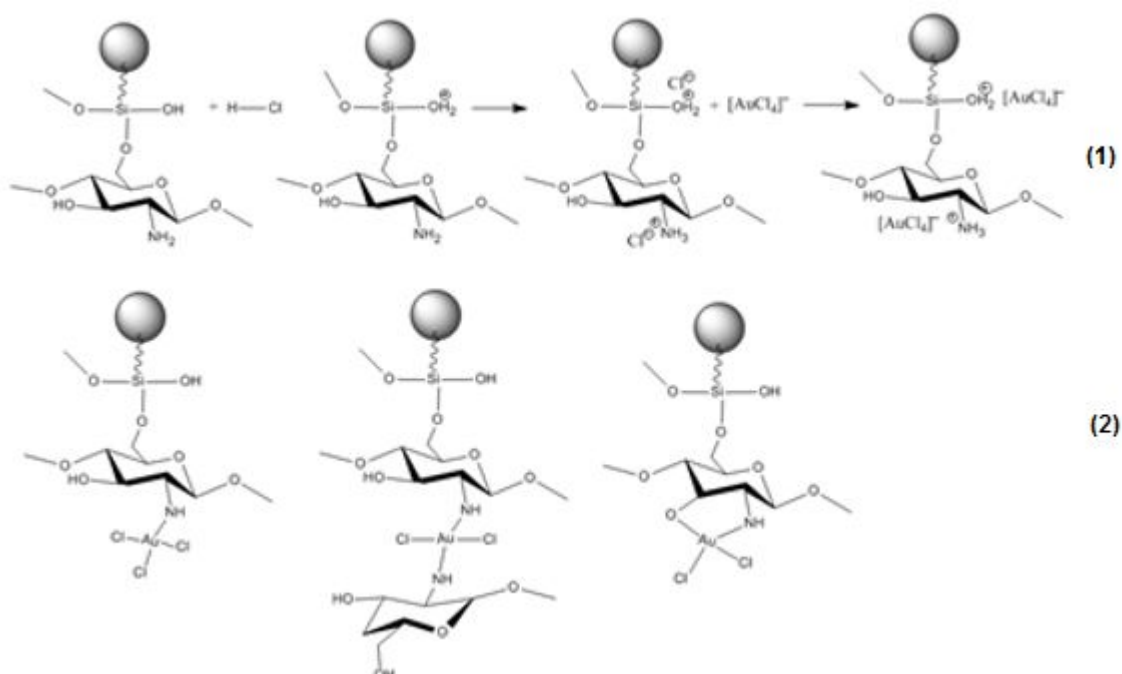


Fig 11. Possible interaction between MMSC with  $[\text{AuCl}_4]^-$  (1) ion-exchange and electrostatic interaction (2) complexation

results of the product indicate that modification silica coated on MM using chitosan has been successfully performed with weight ratio between inorganic material (MMS) and chitosan is 2.5:1.

#### Adsorbent Stability

The stability test of the adsorbent was evaluated based on the solubility of iron and chitosan in MMSC at various pHs (1 to 6). Percentage of iron dissolved from the adsorbent is shown in Fig. 7. At pH 1-2 the Fe ion dissolved from MM is higher than MMS and MMSC. At pH of 3-6 the percentage of iron released from MM, MMS, and MMSC are not different significantly with relative low percentage. Modification of MM surface

using silica and chitosan prevents the protonation of amine groups and causes low solubility. Under acidic condition (pH 1-2) after chitosan dissolved, the acid solution contacts to the silica and forms  $\text{Si}(\text{OH})_4$  leading to break Fe-O-Si bond. The surface of the magnetic material that is not protected contacts directly to the acid, and make iron ion to dissolve.

The adsorbent stability may be examined by measuring the chitosan dissolved at various pHs with UV-Vis spectrometer and calculated weight percent of chitosan that dissolved. Absorbance measurement was carried out on the supernatant of MMSC suspension at maximum absorbance at 282 nm. Percent weight of dissolved chitosan was calculated with gravimetry

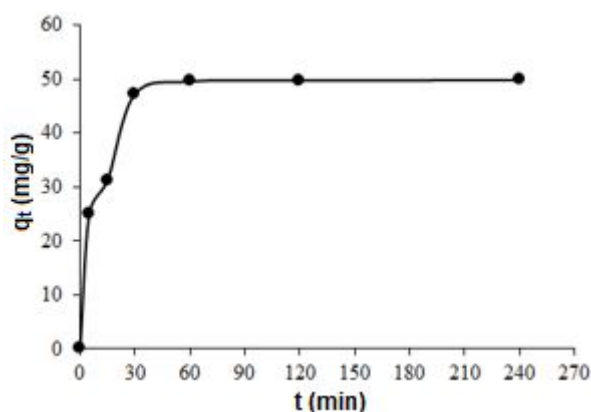


**Fig 12.** Effect of contact time of Au(III) adsorption by MMSC

method by measured weight of 20 mg adsorbent before and after solvation treatment. Absorbance of each sample at various pH is shown in Fig. 8. The absorbance of MMSC was relative high at pH 1 and decreased along with pH increasing. At pH 4-6 the absorbances of the products are not different significantly indicating that product is stable in this range of pH. Weight percent of dissolved chitosan is presented in Fig. 9. The amount of chitosan that dissolved at pH 5 and 6 is the least, which indicate adsorbent is stable at this pH.

#### Adsorption of Au(III)

**Effect of pH.** The important factor that has to be considered to identify the interaction of adsorbent and metal adsorbate is acidity (pH). The acidity of medium affects the charge of adsorbent surface and stability of adsorbent. Moreover, acidity changes metal ion species. Effect of pH to the percentage of Au(III) adsorbed is presented in Fig. 10. Adsorption Au(III) on MMSC increased from pH 1-4, reached maximum at pH 5 and decreased slightly at pH 6. This can be explained that at pH 5  $H^+$  ion in solution protonate  $-NH_2$  and  $-OH$  groups in chitosan. At pH 5 gold ions have a negative charge (as  $[AuCl_3(OH)]^-$ ,  $[AuCl_2(OH)_2]^-$  and  $[AuCl(OH)_3]^-$  species [29], so that the protonated  $-NH_2$  and  $-OH$  are able to absorb the gold ions in solution. The amount of Au(III) that were adsorbed at pH 1 and 2 tends to be low, due to the competition between  $[AuCl_4]^-$  with  $Cl^-$  of HCl. Percentage of adsorbed Au(III) at pH 6 decreased because not all of the active sites of the adsorbent is protonated, leading to weak interaction of adsorbent and adsorbate. Possible interaction between chitosan and Au(III) may occur via ion-exchange, coordination, reduction [26] and electrostatic [14]. Possible interaction between MMSC and Au(III) is shown in Fig. 11.

#### Adsorption kinetics

The effect of contact time on Au(III) adsorption by MMSC is illustrated in Fig. 12. It was observed that

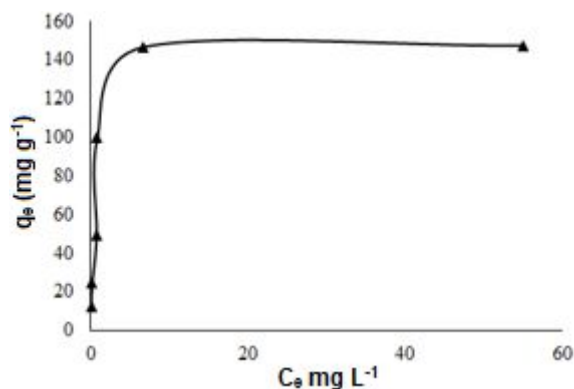


**Fig 13.** Effect of initial metal ion concentration on Au(III) adsorption by MMSC

metal ion adsorption increases with contact time and reaches maximum at 60 min. After 60 min Au(III) adsorption tends to achieve equilibrium. It is clearly stated that adsorption is fast at the beginning due to availability of large amount of active binding sites on the adsorbent. As the amount of active sites decreases, uptake rate of metal is controlled by rate transportation of the adsorbate from the exterior to the interior sites.

Adsorption rate constant ( $k$ ) is one of the important parameters in the study on adsorption kinetics. In this study  $k$  is determined by applying pseudo-first order (Lagergren) and pseudo-second order (Ho) kinetics models. Parameters of kinetic adsorption are presented in Table 3. Adsorption kinetic model was determined based on the value of coefficient linearity ( $R^2$ ). Kinetic parameters data in Table 3 show that the adsorption of Au(III) on MMSC follows the pseudo-second order kinetic model. The  $R^2$  of pseudo-second order is higher than the pseudo-first order model. Additionally, the theoretical value of  $q_e$  in pseudo-second order kinetic model is closer to the experimental one.

#### Adsorption Isotherm

The effect of initial concentration on Au(III) adsorption by MMSC has been studied by keeping other parameters (like pH, dose of adsorbent, and contact time) constant, and the data is expressed in Fig. 13. The initial metal ion concentration provides an important driving force to overcome all mass transfer resistance of the metal between aqueous and solid phase [30]. Based on the results it can be revealed that as the initial metal ion concentration increases the percentage removal of Au(III) decreases. At low concentration of metal ion the active binding sites of adsorbent remains unsaturated offering large surface area for metal ion adsorption while at higher concentration accumulation of adsorbent particles leads

**Table 3.** Pseudo first order and pseudo second order rate constants for Au(III) adsorption on MMSC

Material	Pseudo-1 order			Pseudo-2 order		
	$k_1$ ( $\text{min}^{-1}$ )	$q_e$ ( $\text{mg g}^{-1}$ )	$R^2$	$k_2$ ( $\text{g mg}^{-1} \text{min}^{-1}$ )	$q_e$ ( $\text{mg g}^{-1}$ )	$R^2$
MMSC	$2.59 \times 10^{-2}$	50.426	0.988	$4.10 \times 10^{-3}$	51.020	0.999

**Table 4.** Langmuir and Freundlich parameters for the adsorption of Au(III) on MMSC

Material	Langmuir Parameters			Freundlich Parameters		
	$R^2$	$q_{\text{max}}$ ( $\text{mg g}^{-1}$ )	$K_L$ ( $\text{L mg}^{-1}$ )	$R^2$	KF ( $\text{mg g}^{-1}$ )	n
MMSC	0.9995	149.2	1.20	0.7930	51.71	2.6

to the decrease in total surface area of the adsorbent. The relationship between the amount of substance adsorbed per unit mass of adsorbent at constant temperature and its concentration in the equilibrium solution is called as adsorption isotherm. The equilibrium adsorption isotherms are important in determining the adsorption capacity of Au(III) adsorption onto MMSC. The experimental data is fitted into the Langmuir and Freundlich isotherm models.

Parameters of Langmuir and Freundlich isotherm models for on Au(III) adsorption by MMSC are shown in Table 4. Freundlich isotherm is determined based on the equilibrium relation between the surface of heterogeneous adsorbent and adsorbate. The high  $K_F$  value (Freundlich constant) presents the easiness of adsorption process in solution [31]. Langmuir adsorption isotherm is examined based on the adsorbent monolayer surface and all sides of the active surface of the adsorbent give the same affinity to interact with adsorbate.  $K_L$  value (Langmuir constant) relates to the adsorption energy. The higher of the  $K_L$  value indicates the increasing affinity of adsorbate to the adsorbent. The correlation coefficients obtained from the Langmuir and Freundlich plots are 0.9995 and 0.793, respectively. The higher correlation coefficient  $R^2$  value indicates the better fit and applicability of Langmuir isotherm model to the adsorption experimental data, with adsorption capacity of  $149.254 \text{ mg g}^{-1}$ . The  $q_{\text{max}}$  value of each of these adsorbents is greater than the unmodified modified capacity of BM-silica adsorption which is only  $15.945 \text{ mg g}^{-1}$ . The adsorption capacity of MMSC is also greater when compared with adsorption capacity of magnetic-chitosan (17) and cotton fiber/chitosan (14).

## CONCLUSION

The present study shows that modification of silica coated on iron sand magnetic materials with chitosan via sol-gel method has been successfully carried out. The product showed as an effective adsorbent for Au(III) from aqueous solution. Hysteresis curve of MMSC showed magnetic property so that the adsorbent can be separated easily from solution with external magnet field.

It was observed that Au(III) adsorption on MMSC was maximum at pH 5 and contact time of 60 min with the adsorption capacity (based on Langmuir isotherm adsorption model) is  $149.3 \text{ mg}$  of adsorbate/g of adsorbent. Study of kinetics revealed a fitted model for pseudo second order with the adsorption constant of  $4.10 \times 10^{-3} \text{ g mg}^{-1} \text{ min}^{-1}$ . Further study regarding to desorb Au(III) from the adsorbent is interesting for further study to confirm the appropriateness of the adsorbent for recovery application of gold.

## ACKNOWLEDGEMENT

The authors are thankful to Ministry of Research, Technology and Higher Education of The Republic of Indonesia for the financial support.

## REFERENCES

- [1] De La Calle, I., Pena-Pereira, F., Cabaleiro, N., Lavilla, I., and Bendicho, C., 2011, Ion pair-based dispersive liquid-liquid microextraction for gold determination at ppb level in solid samples after ultrasound-assisted extraction and in waters by electrothermal-atomic absorption spectrometry, *Talanta*, 84 (1), 109–115.
- [2] Rusdiarso, B., 2007, Studi ekstraksi pelarut emas (III) dalam larutan konsentrat tembaga PT Freeport dengan 8-metylxantin, *BMIPA*, 17 (2), 15–22.
- [3] Sahoo, P.R., and Venkatesh, A.S., 2015, Constraints of mineralogical characterization of gold ore: Implication for genesis, controls and evolution of gold from Kundarkocha gold deposit, Eastern India, *J. Asian Earth Sci.*, 97, 136–149.
- [4] Rubcumintara, T., 2015, Adsorptive recovery of Au(III) from aqueous solution using modified bagasse biosorbent, *Int. J. Chem. Eng. Appl.*, 6 (2), 95–100.
- [5] Kraus, A., Jainae, K., Unob, F., and Sukpirom, N., 2009, Synthesis of MPTS-modified cobalt ferrite nanoparticles and their adsorption properties in

- relation to Au(III), *J. Colloid Interface Sci.*, 338 (2), 359–365.
- [6] Hastuti, S., Nuryono, and Kuncaka, A., 2015, L-arginine-modified silica for adsorption of gold(III), *Indones. J. Chem.*, 15 (2), 108–115.
- [7] Mortazavi, K., Ghaedi, M., Roosta, M., and Montazerzohori, M., 2012, Chemical functionalization of silica gel with 2-((3-silylpropylimino) methyl) phenol (spimp) and its application for solid phase extraction and preconcentration of Fe(III), Pb(II), Cu(II), Ni(II), Co(II) and Zn(II) ions, *Indian J. Sci. Technol.*, 5 (1), 1893–1900.
- [8] Budnyak, T.M., Pylypchuk, I.V., Tertykh, V.A., Yanovska, E.S., and Kolodynska, D., 2015, Synthesis and adsorption properties of chitosan-silica nanocomposite prepared by sol-gel method, *Nanoscale Res. Lett.*, 10 (87), 1–10.
- [9] Jal, P.K., Patel, S., and Mishra, B.K., 2004, Chemical modification of silica surface by immobilization of functional groups for extractive concentration of metal ions, *Talanta*, 62 (5), 1005–1028.
- [10] Karimnezhad, K., and Moghimi, A., 2014, Extraction of Zn(II) using magnetic chitosan nanoparticles grafted with  $\beta$ -cyclodextrin and determination by FAAS, *Orient. J. Chem.*, 30 (1), 95–103.
- [11] Nuryono, Indriyanti, N.Y., Manuhutu, J.B., Narsito, and Tanaka, S., 2013, Sorption of Au(III) and Ag(I) on Amino- and Mercapto-silica hybrid columns, *J. Anal. Sci.*, 17, 244–245.
- [12] Hamoudi, S., El-Nemr, A., Bouguerra, M., and Belkacemi, K., 2012, Adsorptive removal of nitrate and phosphate anions from aqueous solutions using functionalized SBA-15: Effects of the organic functional group, *Can. J. Chem. Eng.*, 90 (1), 34–40.
- [13] He, X., Xu, H., and Li, H., 2015, Cr(VI) removal from aqueous solution by chitosan/carboxymethyl cellulose/silica hybrid membrane, *World J. Eng. Technol.*, 3, 234–240.
- [14] Qu, R., Sun, C., Wang, M., Ji, C., Xu, Q., Zhang, Y., and Yin, P., 2009, Adsorption of Au(III) from aqueous solution using cotton fiber/chitosan composite adsorbents, *Hydrometallurgy*, 100 (1-2), 65–71.
- [15] Dhawade, P., and Jagtap, R., 2012, Comparative study of physical and thermal properties of chitosan-silica hybrid coatings prepared by sol-gel method, *Chem. Sin.*, 3 (3), 589–601.
- [16] Mohamed, M.A., Mulyasuryani, A., and Sabarudin, A., 2013, Adsorption of cadmium by silica chitosan, *J. Pure Appl. Chem. Res.*, 2 (2), 62–66.
- [17] Chang, Y., Chen, D., and Chen, D., 2006, Recovery of gold(III) ions by a chitosan-coated magnetic nano-adsorbent, *Gold Bull.*, 39 (3), 98–102.
- [18] Cornell, R.M., and Schwertmann, U., 2003, *The Iron Oxides: Structure, Properties, Reactions, Occurrences and Uses*, 2<sup>nd</sup> Ed., Wiley.
- [19] Ho, S.H., 2004, Citation review of Lagergren kinetic rate equation on adsorption reactions, *Scientometrics*, 59 (1), 171–177.
- [20] Wang, L., Peng, H., Liu, S., Yu, H., Li, P., and Xing, R., 2012, Adsorption properties of gold onto a chitosan derivative, *Int. J. Biol. Macromol.*, 51 (5), 701–704.
- [21] AbdElhady, M.M., 2012, Preparation and characterization of chitosan/zinc oxide nanoparticles for imparting antimicrobial and UV protection to cotton fabric, *Int. J. Carbohydr. Chem.*, 2012, 1–6.
- [22] Ren, Y., Abbood, H.A., He, F., Peng, H., and Huang, K., 2013, Magnetic EDTA-modified chitosan/SiO<sub>2</sub>/Fe<sub>3</sub>O<sub>4</sub> adsorbent: Preparation, characterization, and application in heavy metal adsorption, *Chem. Eng. J.*, 226, 300–311.
- [23] Xi, F., Wu, J., and Lin, X., 2006, Novel nylon-supported organic-inorganic hybrid membrane with hierarchical pores as a potential immobilized metal affinity adsorbent, *J. Chromatogr. A*, 1125 (1), 38–51.
- [24] Shirosaki, Y., Tsuru, K., Hayakawa, S., Osaka, A., Lopes, M.A., Santos, J.D., and Fernandes, M.H., 2005, In vitro cytocompatibility of MG63 cells on chitosan-organosiloxane hybrid membranes, *Biomaterials*, 26 (5), 485–493.
- [25] Lei, Z., Pang, X., Li, N., Lin, L., and Li, Y., 2009, A novel two-step modifying process for preparation of chitosan-coated Fe<sub>3</sub>O<sub>4</sub>/SiO<sub>2</sub> microspheres. *J. Mater. Process. Technol.*, 209 (7), 3218–3225.
- [26] Dongre, R., Thakur, M., Ghugal, D., and Meshram, J., 2012, Bromine pretreated chitosan for adsorption of lead(II) from water, *Bull. Mater. Sci.*, 35 (5), 875–884.
- [27] Liu, W., Yin, P., Liu, X., Dong, X., Zhang, J., and Xu, Q., 2013, Thermodynamics, kinetics, and isotherms studies for gold(III) adsorption using silica functionalized by diethylenetriamine methylenephosphonic acid, *Chem. Eng. Res. Des.*, 91 (12), 2748–2758.
- [28] Pylypchuk, I.V., Kołodyńska, D., Kozioł, M., and Gorbyk, M.M., 2016, Gd-DTPA adsorption on chitosan/magnetite nanocomposites, *Nanoscale Res. Lett.*, 11 (168), 1–10.
- [29] Paclawski, K., and Fitzner, K., 2004, Kinetics of gold(III) chloride complex reduction using sulfur(IV), *Metall. Mater. Trans. B*, 35, 1071–1085.
- [30] Pestov, A., Nazirov, A., Modin, E., Mironenko, A., and Bratskaya, S., 2015, Mechanism of Au(III)

reduction by chitosan: Comprehensive study with  $^{13}\text{C}$  and  $^1\text{H}$  NMR analysis of chitosan degradation products, *Carbohydr. Polym.*, 117, 70–77.

[31] Patel, P.A., Eckart, J., Advincula, M.C., Goldberg, A.J., and Mather, P.T., 2009, Rapid synthesis of polymer-silica hybrid nanofibers by biomimetic mineralization, *Polymer*, 50 (5), 1214–1222.